Am J Nucl Med Mol Imaging 2025;15(6):251-261
www.ajnmmi.us /ISSN:2160-8407/ajnmmi0162258

*Original Article*

# Quantification of I-131 thyroid remnant uptake in patients with thyroid cancer

Elaheh Amini[1], Catherine Kim[2], Asya S Al-Busaidi[3], Ran Klein[1,4,5], Wanzhen Zeng[4,5]

*[1]Systems and Computer Engineering, Carleton University, Ottawa, Ontario, Canada; [2]Faculty of Medicine, University of Ottawa, Ottawa, Ontario, Canada; [3]Department of Radiology and Nuclear Medicine, Sultan Qaboos Comprehensive Cancer Care and Research Centre, University Medical City, Muscat, Oman; [4]Division of Nuclear Medicine and Molecular Imaging, Faculty of Medicine, University of Ottawa, Ottawa, Ontario, Canada; [5]Division of Nuclear Medicine and Molecular Imaging, Department of Medicine, The Ottawa Hospital, Ottawa, Ontario, Canada*

Received November 25, 2024; Accepted June 15, 2025; Epub December 15, 2025; Published December 30, 2025

**Abstract:** Radioiodine ablation is commonly performed after thyroidectomy for well-differentiated thyroid cancer (DTC). This study aimed to quantify thyroid remnant uptake in standardized uptake values (SUV) and evaluate its correlation with post-therapy Thyroglobulin (Tg) levels across different risk groups. We retrospectively quantified SUV uptake with attenuation, scatter, and resolution recovery corrections on post-therapy SPECT/CT in thyroid cancer patients referred to our centre between 2015 and 2017. Thyroid remnant was segmented with a maximum SUV of 0.5 as the threshold and total thyroid remnant uptake ($SUV_{total}$) was obtained. Patients were stratified into low-intermediate, high-intermediate, and high-risk groups based on clinical risk and therapeutic dose. The primary outcome was the correlation between $SUV_{total}$ and post-therapy Tg levels. The cohort consisted of 174 adults (age: 50.7±16.0 yr, F:M=110:64). Moderate correlations were found between $SUV_{total}$ and Tg levels in low-intermediate and high-intermediate groups (Spearman's $\rho$=0.65, P<0.001; $\rho$=0.61, P<0.001, respectively). No significant correlation was found in the high-risk group ($\rho$=0.12, P=0.33). Stimulated Tg levels increased (median Tg: 4, 7, and 13 pmol/L) and thyroid remnant uptake decreased (median $SUV_{total}$: 272, 51, and 33) across the low-intermediate, high-intermediate, and high risk groups. In conclusion, this study shows good correlations between the thyroid remnant uptake and thyroglobulin in subgroups of patients with low-intermediate and high-intermediate risk DTC. The rationales for lack of significant correlation in the high-risk group DTC were discussed. Thyroid uptake quantification may serve as a feasible substitute for Tg measurements in post-ablation follow-up, offering potential for predicting disease recurrence.

**Keywords:** Thyroid cancer, thyroid remnant quantification, radioiodine ablation therapy, Single-photon emission computed tomography (SPECT)/CT, standard uptake value (SUV)

## Introduction

In patients with intermediate- and high-risk thyroid cancer following total thyroidectomy, radioactive iodine (RAI) therapy with $^{131}$I sodium iodine ($^{131}$I NaI) is recommended by clinical guidelines for thyroid remnant ablation and adjuvant therapy [1, 2]. Subsequently, these patients are monitored through thyroglobulin (Tg) measurements, diagnostic whole-body radioiodine thyroid scans, and/or radiological imaging.

Post-RAI therapy images are routinely acquired using hybrid single photon emission computed tomography/computed tomography (SPECT/CT) of the neck and upper chest, in addition to traditional whole-body planar imaging. Although the routine assessment of the thyroid remnant is primarily visual, recent advancements in image reconstruction software now enable us to quantify the thyroid remnant uptake, which is one of the primary goals of the current study. With the quantified remnant activity, a direct correlation with serum Tg level is possible, potentially providing insight into the association between the neck uptake on imaging and serum Tg at the time of RAI irradiation.

Tg is a large glycoprotein produced by normal or well-differentiated malignant thyrocytes [3]. It acts as a substrate for the synthesis of thyroid hormones. Tg is synthesized exclusively in the thyroid follicular cells as a precursor to thyroid hormones and is subsequently metabolized in the liver, with a mean elimination half-life of 65.2 h [4, 5]. In patients following thyroidectomy and RAI therapy, Tg is an important tumor marker for disease progression.

The risk of thyroid remnant ablation failure may be related to the treatment dose, although this conclusion remains debatable [6, 7]. Serum Tg levels have been shown to correlate well with the tumor burden [8], and post-ablation Tg levels have been identified as potential predictors of thyroid remnant ablation failure [9-11] and therapeutic failure [12, 13]. A study in patients treated with 150 mCi of $^{131}$I NaI found that delayed whole-body scan neck counts correlated with serum Tg levels, and both were significant factors for predicting ablation success [14]. Nevertheless, there are limited studies exploring the relationship between Tg (both suppressed and stimulated) and thyroid remnant uptake quantified in standardized uptake values (SUV).

Approximately 10-25% of patients with differentiated thyroid cancer have positive thyroglobulin antibodies (TgAb) measurements [15, 16], which can interfere with the Tg measurement, potentially leading to underestimation or possibly overestimation of Tg levels. Therefore, in this subgroup of the patient population, measuring the uptake in the thyroid remnant may provide an important surrogate marker for Tg levels. In addition, quantification of radioiodine-avid lesions could serve as a surrogate marker for Tg levels in monitoring disease recurrence during long-term follow-up, and possibly help to determine the optimal $^{131}$I NaI ablation dose in disease recurrence.

In this study, we aimed to (1) quantitatively measure thyroid remnants uptake on SPECT/CT images, and (2) assess the correlation between thyroid remnants uptake and Tg levels measured immediately following the ablation.

## Materials and methods

This work outlines the collection of a dataset from patients who underwent RAI therapy following total thyroidectomy at our Nuclear Medicine clinic for post-treatment monitoring. It details the image reconstruction process and thyroid remnant quantification and concludes with a description of the statistical tests employed to assess the significance of our findings.

*Subjects*

A retrospective chart and imaging review was conducted of adult patients with differentiated thyroid cancer (DTC) referred to our clinic for radioactive iodine ablation therapy following thyroidectomy from 2015 to 2017. After reviewing the electronic medical records of this study group, including disease history, pathology, and laboratory results through the electronic medical records, we excluded patients who had missing body weight records, missing stimulated Tg levels, known distal metastases, no SPECT/CT of the neck, or positive anti-Tg antibodies at the time of treatment. Additionally, patients with distal metastases detected on post-RAI therapy imaging were excluded. The limited number of patients with thyroid stimulation induced by hormone withdrawal were also excluded, as Tg levels behave differently in this group compared to those induced by Thyrogen (thyroid stimulating hormone (TSH)) stimulation [17, 18].

At our institution, Tg and TgAb levels are usually measured around the time of RAI therapy under Thyrogen stimulation, typically pre-Tg was measured 2 days before RAI therapy and post-Tg was measured 2 days after RAI therapy, or thyroid hormone withdrawal stimulation (2 days after RAI). RAI therapy for our study group was typically performed more than 6 weeks following the surgery [19]. Patients with TgAb levels below the reference threshold, defined as ≤22 kIU/L or ≤40 kIU/L depending on the lower cut-off value of the immunoassay method used by the reporting laboratory, were considered 'antibody-negative' and included in the study population.

*I-131 Sodium Iodine SPECT/CT imaging*

Post-ablation $^{131}$I NaI SPECT/CT images were acquired using SPECT with low-dose CT on Siemens Symbia T or Siemens Intevo Bold scanners with high-energy parallel hole collimators, reconstructed using ordered subset expectation maximization (OSEM) with attenuation, scatter, and resolution recovery corrections, as well as absolute quantification calibration, using HybridRecon™ 5.0 (Hermes Medical Solutions, Stockholm, Sweden). The reconstructed images were visualized, and the areas attributed to thyroid remnant tissues were segmented and quantified using the Affinity Viewer 4.0 software (Hermes Medical Solutions, Stockholm, Sweden, 2023). Given the minimal background uptake in the neck outside of thyroid remnants, with a mean of 0.043±0.06 $SUV_{max}$ observed in this study, a thresholding-based segmentation method was applied to each SPECT image. Regions with activity uptake exceeding an arbitrary threshold of 0.5 $SUV_{max}$, which is roughly an order of magnitude higher than the background uptake, were delineated as potential thyroid remnants in most patients. We retained areas with activity uptake greater than 0.5 $SUV_{max}$ that corresponded to the thyroid tissue while excluding other regions such as the parotid glands. After delineating the remnant thyroid tissue, we recorded the $SUV_{max}$, $SUV_{mean}$, volume (ml), and $SUV_{total}$ of the segmented thyroid remnants (**Figure 1**). In cases where the background activity exceeded 0.5 $SUV_{max}$, a spherical constraint was applied at the thyroid bed to facilitate the exclusion of non-target tissues. To test the robustness of the results, we repeated all thyroid remnant segmentations using a $SUV_{max}$ cut-off of 0.1 to capture more thyroid remnants.

The concept of $SUV_{total}$ is similar to total lesion glycolysis (tumor burden) in oncology, borrowed from FDG PET quantification. It is calculated by multiplying the $SUV_{mean}$ of the segmented remnant tissue by its volume and provides a measure of the functional activity of our target area.

To perform a detailed analysis, the patients were divided into low-intermediate, high-intermediate, and high-risk groups according to Cancer Care Ontario guidelines [20]. Prior to RAI therapy, all patients were consulted, and the administered treatment dose was determined based on clinical, histopathological, and imaging information. We used the above clinically determined therapy doses as surrogates to reclassify each patient into the corresponding risk group in the context of this study.

*Statistical analysis*

To select the appropriate statistical analysis tool, we used the Shapiro-Wilk test to assess the normality of our mea-

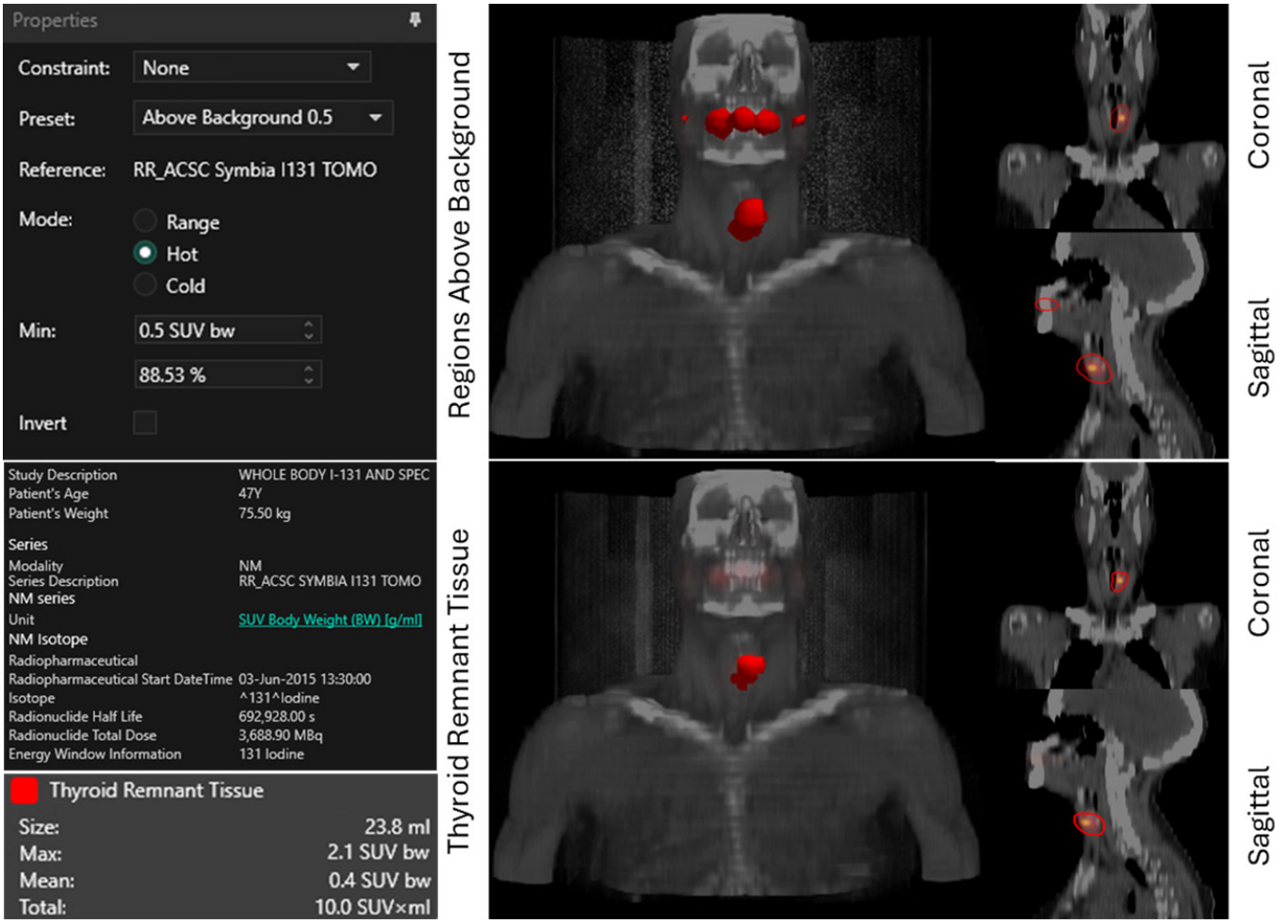


**Figure 1.** Example demonstrating the process of segmentation and quantification of thyroid remnant tissue. All images display the SPECT scan co-registered with the corresponding CT in a 3D rendering, along with single slices in the coronal and sagittal views. *Top row*: We performed the segmentation on the SPECT image using threshold criteria (>0.5 $SUV_{max}$) via the Single Click Segmentation tool in Affinity Viewer. After setting the threshold value, a preview of the threshold region was generated from all available voxels that met the criteria. *Bottom row*: We selected the regions associated with the thyroid tissue, after which region statistics were automatically calculated. If multiple disconnected regions were selected, we merged them before recording the final statistics. Additional study properties, including the patient's weight and administered dose, are also shown.

surements across all risk groups. To assess the statistical significance of measurement differences between risk groups, we used the Kruskal-Wallis test. If a significant difference was found between risk groups for a measurement, post-hoc pairwise comparisons were performed using the Mann-Whitney test to identify pairs responsible for the difference. In these cases, the Bonferroni correction was applied to *p*-values to adjust for multiple comparisons between risk groups. The significance level was set at 0.05.

The correlation between $SUV_{total}$ and stimulated Tg levels was assessed using Spearman's rank correlation coefficient (ρ), with a *p*-value of less than 0.05 considered statistically significant. The correlation between non-stimulated Tg levels and $SUV_{total}$ was not assessed due to the considerable number of patients with undetectable Tg levels. Other imaging parameters are reported as median (range) unless stated otherwise.

## Results

Initially, we identified 225 patients who had undergone their first RAI therapy following total thyroidectomy. We excluded patients with incomplete data, including those with no documented weight (n=16), no post-therapy Tg measurements (n=9), or no neck SPECT/CT imaging (n=3). In addition, patients who underwent thyroid hormone withdrawal (n=10), had distal metastasis (n=6), or had positive TgAb (n=7) were excluded from the study. This resulted in 174 patients who had undergone Thyrogen-stimulated RAI therapy, used for further analysis in our study (**Figure 2**).

Among the 174 patients, 64 (37%) were men and 110 (63%) were women, with a mean age of 50.7±16.0 years. Histological analysis revealed that 161 (93%) of the patients had papillary thyroid cancer, 9 (5%) had follicular thyroid cancer, and the remaining 4 (2%) had mixed papillary-follicular thyroid cancer.

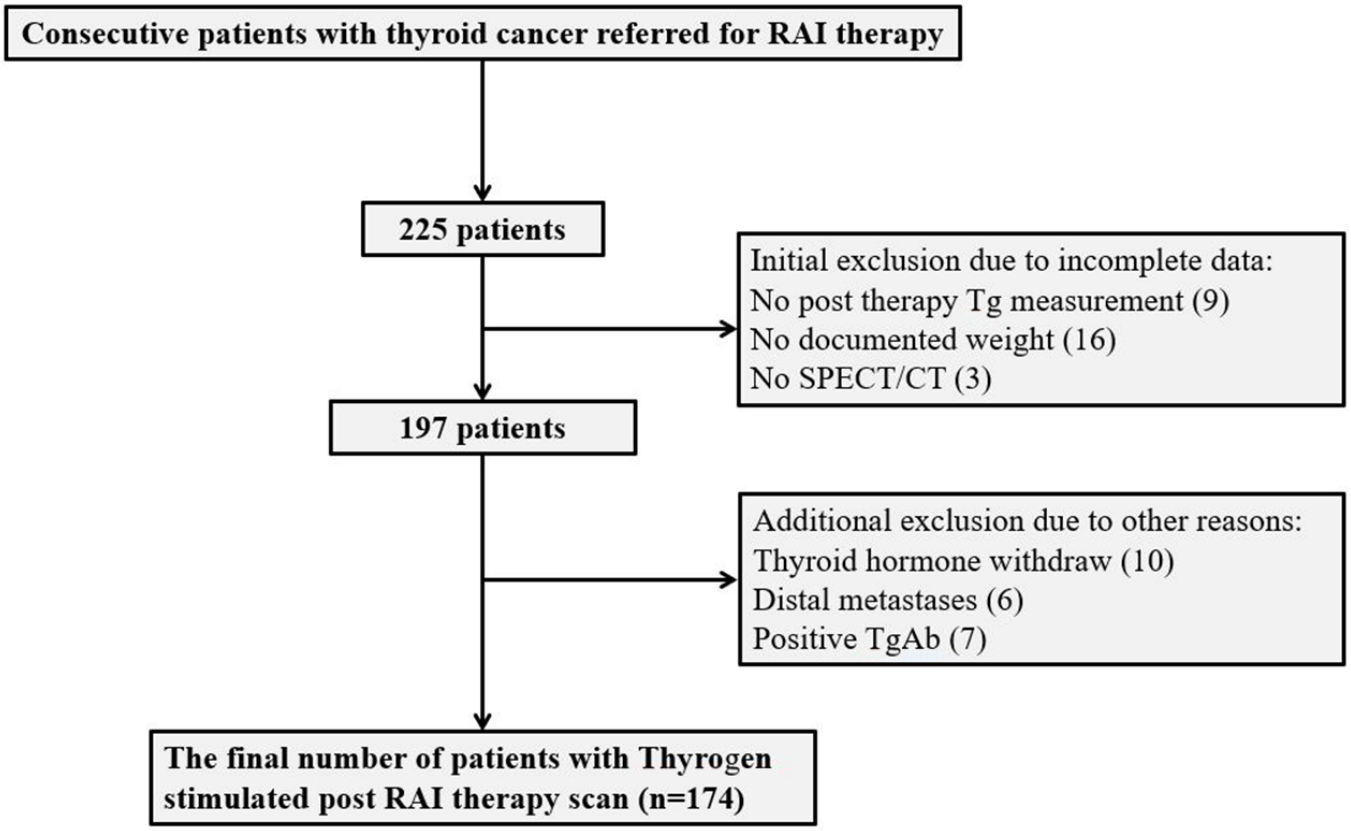


**Figure 2.** Flowchart illustrating the data collection process, including the total number of cases initially collected, the exclusion criteria applied, and the final dataset used for analysis.

**Table 1.** Demographic and clinical characteristics of the study cohort

| Characteristics (n=174) | | Value |
|---|---|---|
| Age at RAI therapy | Years | 50.7±16.0 |
| Gender | Male | 64 (34%) |
| | Female | 110 (66%) |
| Histology | Papillary | 161 (93%) |
| | Follicular | 9 (5%) |
| | Mixed | 4 (2%) |
| Initial risk classification | Low-Intermediate | 58 (33%) |
| | High-Intermediate | 52 (30%) |
| | High | 64 (37%) |
| I-131 Dose | mCi | 90.2±45.9 |
| Pre-ablation Tg (2 days) | pmol/L (n=167) | 0.5 (0.2, 47.3) |
| Post-ablation Tg (2 days) | pmol/L (n=174) | 7.0 (0.2, 531.2) |
| Ratio (post-/pre-ablation Tg) | | 11.0 (1.0, 403.0) |

Values are indicated as mean ± standard deviation, median (minimum, maximum), or number (percentage %). Note: The sensitivity for Tg ranged from 0.2 pmol/L (0.13 μg/L) to 0.76 pmol/L (0.51 μg/L) in hospital and clinic laboratories.

Among the 174 patients, 58 (33%) received doses of 28-75 mCi and were classified as low-intermediate risk, 52 (30%) received 75-110 mCi and were classified as high-intermediate, and 64 (37%) received doses greater than 110 mCi and were classified as high risk. The mean ± standard-deviation pre-ablation Tg level, measured approximately 2 days before RAI therapy, was 1.8±4.9 pmol/L (median: 0.5), while the mean post-ablation Tg level, measured approximately 2 days after RAI therapy, was 32.9±70.4 pmol/L (median: 7.0). The overall ratio between post-ablation and pre-ablation Tg levels was 36.1±74.3 pmol/L (median: 11.0) (**Table 1**).

The imaging data statistics of the thyroid remnant obtained using the segmentation threshold of 0.5 $SUV_{max}$ and stimulated Tg levels are described in **Table 2**. For the low-intermediate, high-intermediate, and high-risk groups, the stimulated Tg (pmol/L) values (median (IQR)) were 3.8 (1.2, 8.7), 7.1 (1.7, 25.3), and 13.4 (3.6, 74.0), with corresponding thyroid remnant activity $SUV_{total}$ values (median (IQR)) of 271.5 (82.9, 665.5), 51.4 (9.8, 138.8), and 33.1 (10.7, 108.5), respectively. A moderate correlation was observed between the $SUV_{total}$ and stimulated Tg levels in the low-intermediate and high-intermediate risk groups, with a Spearman's correlation coefficient of 0.65 ($p$-value <0.001) and 0.61 ($p$-value <0.001), respectively [21]. In contrast, no significant correlation was noted for the high-risk group, with a Spearman's correlation coefficient of

**Table 2.** Correlation of thyroid remnant total uptake with post-therapy Tg levels across risk groups

| | N | Mean Dose (mCi) | $SUV_{total}$ (SUV×ml) | Stimulated Tg (pmol/L) | Spearman's correlation coefficient |
|---|---|---|---|---|---|
| Low-Intermediate | 58 | 31.4±5.1 | 271.5 (82.9, 665.5) | 3.8 (1.2, 8.7) | 0.65* |
| High-Intermediate | 52 | 99.5±3.2 | 51.4 (9.8, 138.8) | 7.1 (1.7, 25.3) | 0.61* |
| High | 64 | 137.9±14.1 | 33.1 (10.7, 108.5) | 13.4 (3.6, 74.0) | 0.12 |

*Indicated P<0.05. Values are indicated as mean ± standard deviation or median (low-quartile, high-quartile).

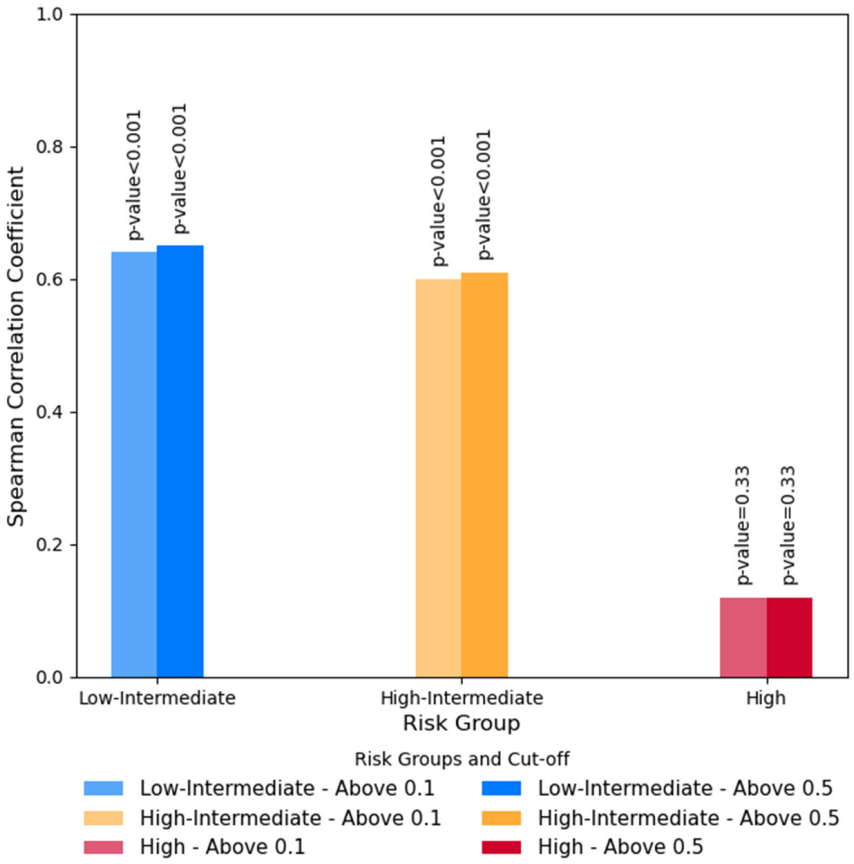


**Figure 3.** Bar graph showing Spearman's correlation coefficients and associated *p*-values between total lesion uptake (using thresholds of 0.1 $SUV_{max}$ and 0.5 $SUV_{max}$) and Tg levels, stratified by risk group.

0.12 (*p*-value =0.33). When considering the entire cohort, a weak but significant correlation was found, with Spearman's correlation coefficient of 0.23 (*p*-value =0.002), highlighting the importance of risk stratification to uncover stronger and more clinically relevant associations that are masked when analyzing the cohort as a whole.

Similar findings are identified using the segmentation threshold of 0.1 $SUV_{max}$, suggesting the robustness of our method to a range of thresholds (**Figure 3**).

Stimulated Tg levels were observed to be low in the low-intermediate risk group (median =3.8) and higher in the high-intermediate (median =7.1) and high-risk (median =13.4) groups, while $SUV_{total}$ was higher in the low-intermediate risk group and decreased in the higher risk groups. In addition, discordant findings were noted between Tg and $SUV_{total}$, with low $SUV_{total}$ and high Tg discordance predominantly observed in the high-risk group, while high $SUV_{total}$ and low Tg discordance were seen exclusively in the low-intermediate risk group (**Figure 4**).

We further examined the differences between Tg measurements and total lesion uptake, focusing on variations across different risk groups. **Figure 5** shows the distribution of Tg measurements after RAI therapy stratified by risk groups. The Tg levels were significantly different between the low-intermediate and high-risk groups (*p*-value <0.001) and low-intermediate and high-intermediate risk groups (*p*-value =0.03). However, no significant difference was observed between the high-intermediate and high-risk groups.

**Figure 6** shows the distribution of total thyroid remnant uptake $SUV_{total}$ measured for both thresholds of 0.1 $SUV_{max}$ and 0.5 $SUV_{max}$ and stratified by risk groups. Significant differences were found between the low-intermediate and high-intermediate risk groups (*p*-values <0.001 for both thresholds of 0.1 and 0.5 $SUV_{max}$) and between the low-intermediate and high-risk groups (*p*-values <0.001, for both 0.1 and 0.5 $SUV_{max}$). However, the difference between the high-intermediate and high-risk groups did not reach significance (*p*-values =0.31, and 0.31 for both thresholds of 0.1 and 0.5 $SUV_{max}$, respectively).

## Discussion

We reconstructed quantitative SPECT/CT images from post-RAI therapy scans and demonstrated that quantification of thyroid remnant function is feasible and straightforward using a simple image thresholding segmentation approach. Consequently, the proposed approach is readily deployable in many clinical settings using SPECT/CT and contemporary image analysis software.

By dividing patients into low-intermediate, high-intermediate, and high-risk groups based on Cancer Care Ontario

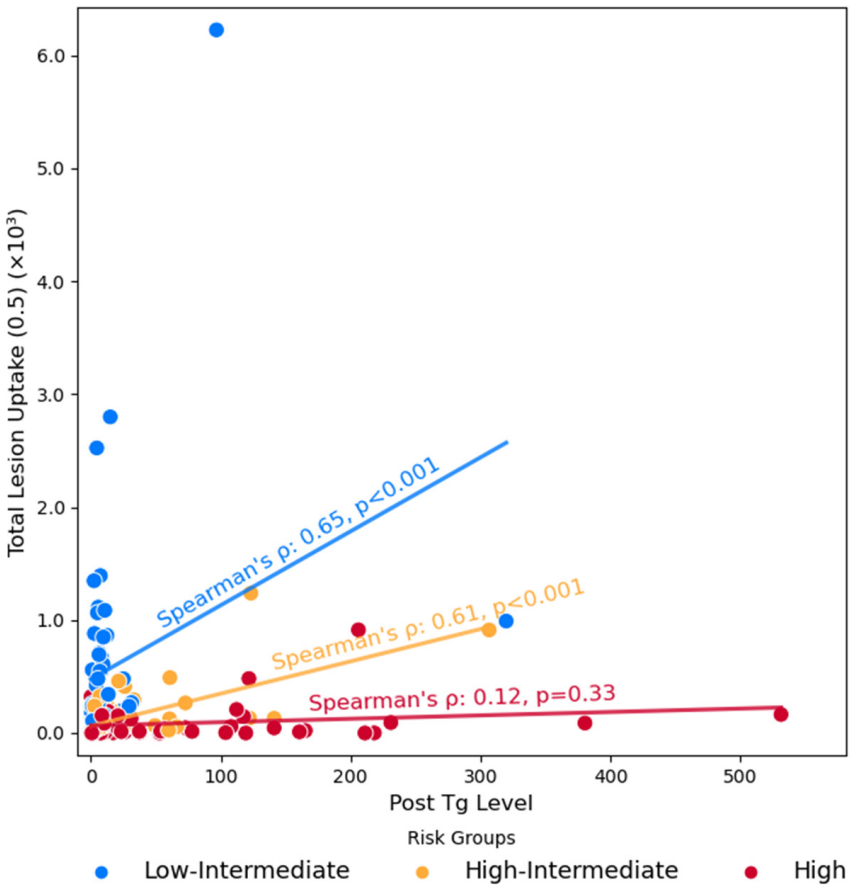


**Figure 4.** Scatter plot demonstrating the relationship between stimulated Tg levels and total lesion uptake (>0.5 $SUV_{max}$) across risk groups. Spearman correlation coefficients and lines of best fit (calculated using least squares regression) are provided for each group. The correlations across risk groups demonstrate varying strengths of association between stimulated Tg levels and total lesion uptake, with stronger relationships in lower-risk groups compared to the high-risk group.

guidelines, we studied the association between thyroid remnant uptake (SUV×ml) and stimulated Tg at the time of radioiodine ablation. The main finding of the study was a moderate correlation between Tg and thyroid remnant $SUV_{total}$ in the low-intermediate and high-intermediate groups (ρ=0.65 and 0.61, with *p*-value <0.001 for both), while no significant correlation was seen in the high-risk group (*p*-value =0.33). However, when considering the entire cohort, a weak but significant positive correlation was found between Tg and $SUV_{total}$ (ρ=0.23, *p*-value =0.002). These results showed that the strength of the association between Tg and $SUV_{total}$ varies across risk categories, with stronger correlations seen in low-intermediate and high-intermediate risk groups compared to the high-risk group, highlighting the importance of risk categorization.

While there are numerous publications on the usefulness of Tg, studies exploring its relationship with the uptake in the thyroid bed post-therapy, are limited. Pre- and post-RAI therapy Tg levels are recognized for aiding in initial risk stratification, guiding adjuvant therapy decisions, and predicting disease recurrence or monitoring treatment failure [2, 9, 22, 23]. For patients at low risk of recurrence, measuring serum Tg at the time of remnant ablation/adjuvant therapy may be useful for predicting subsequent disease-free status [22]. Additionally, postoperative serum Tg levels can be used to predict the likelihood of successful remnant ablation. For instance, stimulated Tg values >5-6 ng/mL measured after thyroid hormone withdrawal were associated with higher rates of ablation failure, whether the administered activity was 30 mCi [9] or 100 mCi [23]. Specifically, a TSH-stimulated Tg >6 ng/mL was associated with a 5-fold increased risk of ablation failure with a 30 mCi administered dose following thyroid hormone withdrawal [9].

In this study, we observed that stimulated Tg (pmol/L) increased (median Tg =4, 7, and 13) while thyroid remnant uptake (SUV×ml) decreased (median $SUV_{total}$ =272, 51, and 33) from the low-intermediate to the high-risk groups. Several factors may presumably contribute to the observation of high Tg and low $SUV_{total}$ in the high-risk group. First, one indication for adjuvant RAI treatment in the high-risk group is to irradiate micrometastases that are not visualized on imaging, in addition to thyroid remnant ablation. Consequently, distal micro-metastatic lesions may contribute to elevated Tg without affecting $SUV_{total}$ in the neck or being visualized on the whole-body scan. Second, the decreased $SUV_{total}$ in the neck may be related to thyroiditis. In a study of patients treated with 150 mCi of $^{131}$I NaI, those with thyroiditis were found to have significantly lower neck counts [14]. Another study involving patients with thyroiditis identified from post-operative specimens prior to RAI therapy reported no or low iodine uptake [24]. In addition, elevated Tg could be secondary to thyroiditis, as several studies have shown that Hashimoto's thyroiditis is correlated with high pre-RAI therapy Tg levels [14, 25]. This finding aligns with the clinical observation of minimal thyroid uptake in patients with subacute thyroiditis on routine thyroid scans. Furthermore, thyroiditis and neck pain may develop following RAI treatment, likely in patients treated with high doses of $^{131}$I NaI and those with significant residual thyroid tissue. Therefore, high Tg levels may result from the release of thyroid hormone due to post-RAI therapy thyroiditis. This is supported by reported cases of transient increases in Tg following RAI therapy, presumed to reflect RAI-induced thyroid tissue destruction/inflammation with subsequent release of Tg from the thyroid remnant [26, 27]. Third, although the patients who underwent RAI therapy had well-differentiated thyroid

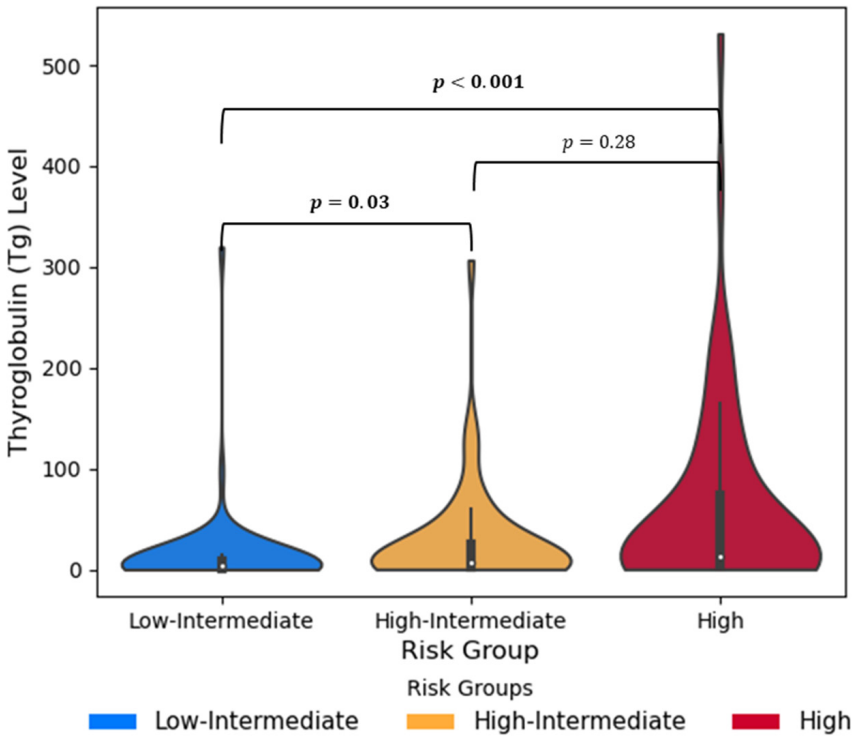


**Figure 5.** Post-ablation Tg measurement (pmol/L) distributions, grouped by risk levels. Modified *p*-values after applying the Bonferroni correction of three are annotated on the figures.

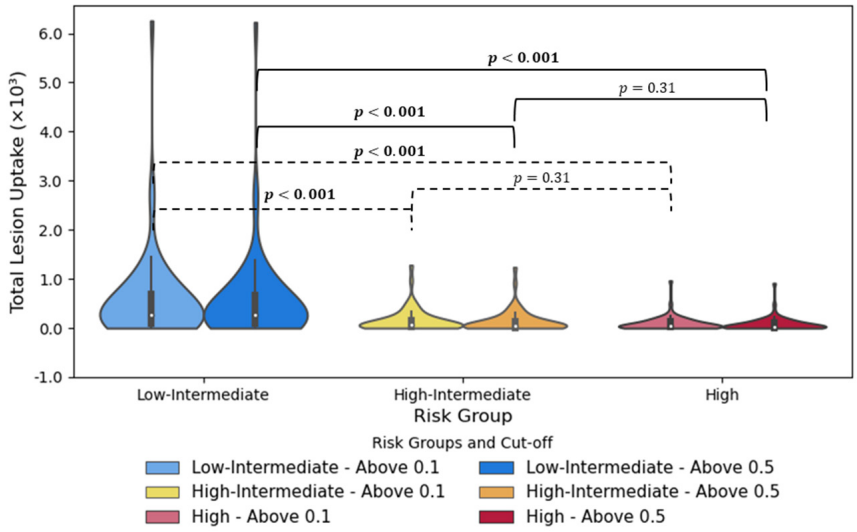


**Figure 6.** Total thyroid remnant uptake measured using two different segmentation thresholds of 0.1 and 0.5 $SUV_{max}$, grouped by risk levels. Modified *p*-values after applying the Bonferroni correction of three are annotated on the figures for each segmentation group.

cancer, certain aggressive histological subgroups (e.g., Hurthle cell cancer, follicular thyroid cancer, columnar cell or tall cell variants, and insular carcinoma) may be less iodine-avid, resulting in lower uptake in the thyroid bed. This is supported by studies showing that aggressive DTC typically demonstrates increased FDG uptake on PET and low uptake on $^{131}$I whole-body scans [28-30]. Furthermore, the loss of the iodine-trapping mechanism in DTC has been observed, leading to the conclusion that an absolute relationship between serum Tg levels and $^{131}$I uptake may not always be evident, as tumors may synthesize Tg but not necessarily trap iodine, and these properties can vary from tumor to tumor [31, 32].

The patient's follow-up was not performed in this study due to the limited sample size and the retrospective nature of the study with the lack of standardized follow-up protocols. Nevertheless, with the understanding of such limitations, we examined the data of the high-risk group (64 patients) 7-9 years after radioiodine ablation therapy. We identified 9 patients with recurrence (14%), 45 with no recurrence, 11 lost to follow-up (17%) and 1 passed away without adequate follow-up. Comparing the recurrent to non-recurrent groups, the difference in median $SUV_{total}$ (42.5 versus 34.3), stimulated Tg (58.6 versus 11.5) and the ratio of Tg (preTg/Stimulated Tg, 18.3 versus 13.9) were not statistically significant. However, the pre-Tg (before Thyrogen stimulation) (2.90 versus 0.76, P<0.005) is statistically significant. This supports the reasoning that distal micrometastases (not visualized on post imaging I-131 scan but producing thyroid hormone) could be a main factor contributing to elevated stimulated Tg, while not contributing to the $SUV_{total}$, which measures thyroid remnant in the neck.

The association between thyroid remnant burden and Tg at the time of radioiodine ablation has been poorly studied or remains controversial. In a study by Hwang et al., neck counts divided into quartiles based on planar images, were reported to increase as Tg levels increased [14]. Conversely, in a study that localized minimal residual RAI uptake in the thyroid bed by SPECT/CT at the time of RAI remnant ablation in 141 DTC patients post-total thyroidectomy, researchers found that residual foci in the thyroid bed had no relationship to postoperative Tg, suggesting that attempts at radical removal of thyroid tissue in these locations may not be warranted [33].

In an earlier study of 317 exams involving 128 patients with DTC, discordant $^{131}$I whole-body scan and Tg findings were observed in 23% of cases [34]. In a more recent

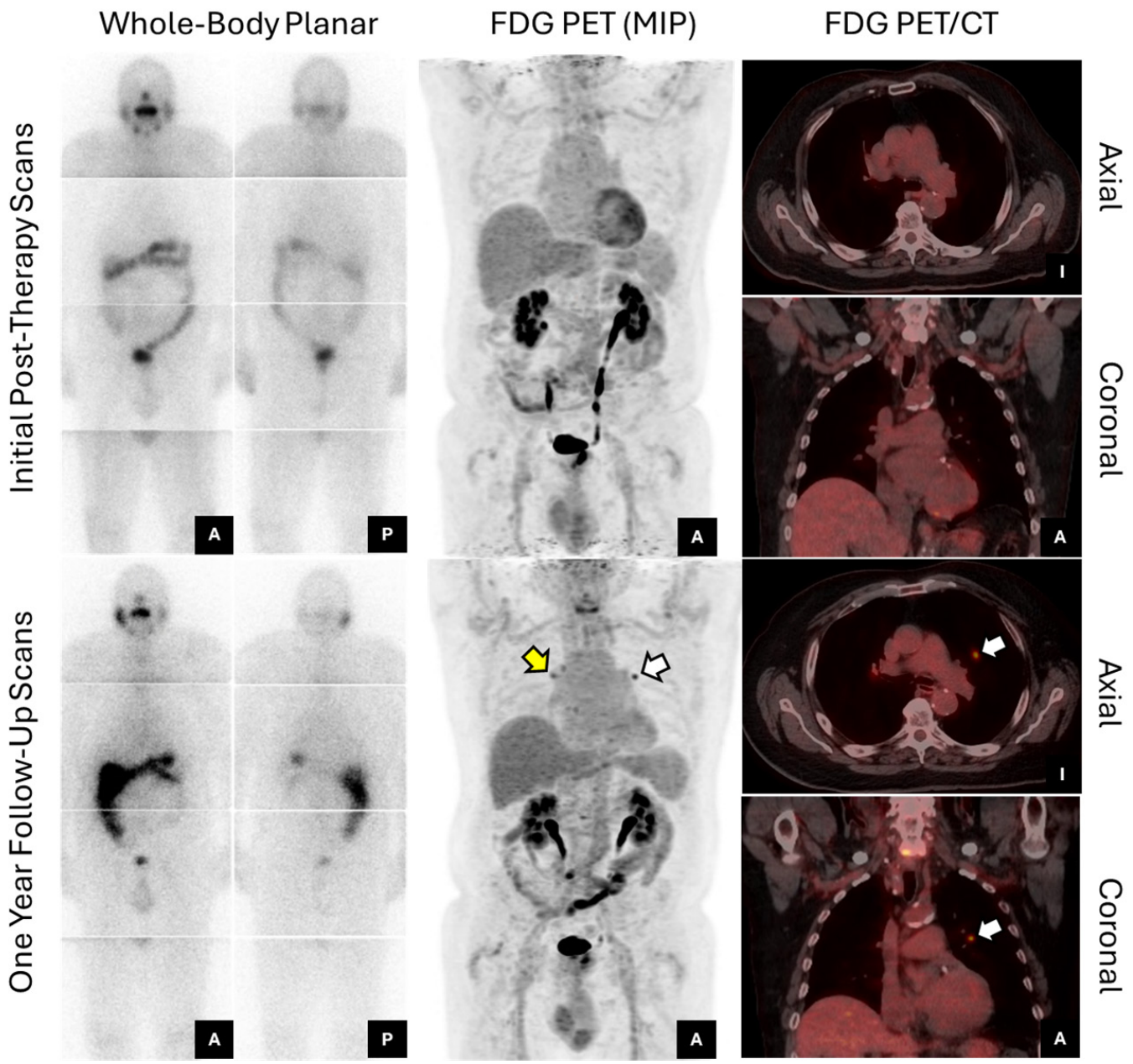


**Figure 7.** Whole-body planar I-131 images (anterior and posterior) and FDG PET (maximum intensity projection (MIP), and axial and coronal slices) for an example patient with pre- and post-stimulated Tg levels of 14.0 pmol/L and 58.6 pmol/L, respectively. Initial post-therapy thyroid scan and FDG PET were negative (top). A year later, follow-up FDG PET revealed lung nodules (white arrows) and a hilar node (yellow arrow), with a stimulated Tg level of 199.7 pmol/L while I-131 post-therapy scan remained negative (bottom).

study involving 84 patients and 170 post-thyroidectomy DTC studies, a high rate of discordant results were found between residual functional tissue and Tg levels (47-55%), and the authors concluded that follow-up should include both Tg assays and imaging studies [35]. Our study suggests that the correlation between Tg and thyroid remnant is dose-dependent and associated with the risk groups, considering the interference of micro-metastases and thyroiditis, which occur predominantly in the high-risk patient group receiving higher treatment doses.

Similar to other publications, outliers were observed in our studies. Interestingly, the discordance of low remnant activity uptake with high Tg (e.g. $SUV_{total}$ <10, Tg>20, n=6, mean dose: 147 mCi) was observed only in the high-risk patient group, whereas the discordance of high remnant activity uptake with low Tg (e.g. $SUV_{total}$ >500, Tg<10, n=18, mean dose: 32.5 mCi) was observed exclusively in the low-intermediate risk group. The rationale for the low remnant activity uptake-high Tg discordance could be the presence of micro-metastases in the high-risk patient group and inflammation in the thyroid bed/remnant due to the high treatment dose. **Figure 7** demonstrates an example from a 76-year-old male with papillary thyroid cancer in the high-risk group, treated with 149.5 mCi (5530 MBq) I-131 NaI. The patient's pre- and post-thera-

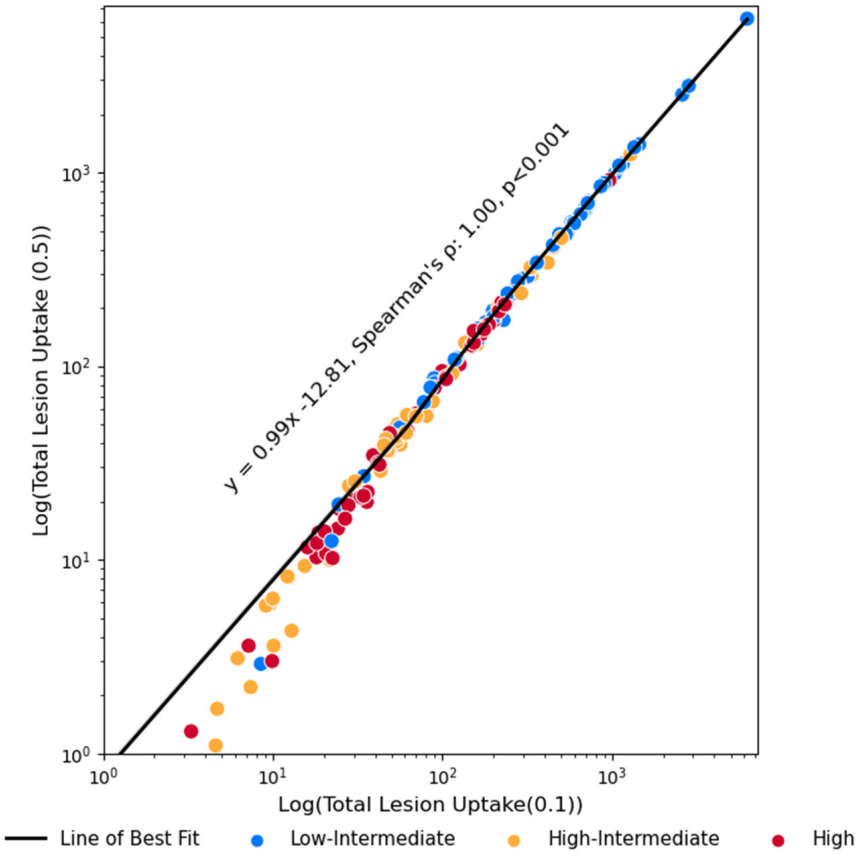


**Figure 8.** Log-log scatter plot demonstrating the strong correlation between total lesion uptake at thresholds of 0.5 and 0.1. The line of best fit, calculated using least squares regression and with a slope of 0.99 highlights this near-perfect association (Spearman's ρ=1.00, P<0.001), indicating consistent proportionality across low, intermediate, and high-risk groups.

py stimulated Tg levels were 14.0 pmol/L and 58.6 pmol/L, respectively. Both post-therapy thyroid scan and FDG PET were initially negative. However, FDG PET one year later revealed two small lung nodules and a hilar node, while the diagnostic thyroid scan with SPECT/CT of the chest remained negative.

The rationale for the high remnant activity uptake-low Tg discordance in the low-intermediate risk group is unclear but could possibly be due to the low sensitivity of the Tg assay in some patients. Tg antibodies are typically measured in conjunction with Tg in each serum sample provided for Tg testing, as TgAb can interfere with Tg immunometric assay measurements. The false-negative Tg results can be attributed to the presence of TgAb, and as such, patients with positive TgAb were excluded from our study. Additionally, varying measurement techniques between labs, the effect of the degree of chronicity of TSH stimulation on serum Tg, and the efficiency of thyroid tissue in secreting Tg may also be contributing factors [32, 35].

Thyroid remnant activity in this study was measured using SPECT/CT with attenuation and scatter corrections, which differs from prior studies that measured counts within the region of interest based on planar images. One limitation of our study is selecting the cut-off criterion for segmenting thyroid remnant activity which has been done somewhat arbitrarily. We selected an $SUV_{max}$ cut-off of 0.5, which is approximately an order of magnitude higher than the average background, to capture remnant activity in the majority of patients. In cases where background activity exceeded the cut-off value, a spherical constraint was placed around the thyroid remnant in the neck, which may have slightly overestimated $SUV_{total}$, but was intended to reflect the contribution of the thyroid remnant. To test the robustness of the results, we repeated all thyroid remnant segmentations using a $SUV_{max}$ cut-off of 0.1 to capture more thyroid remnants. This resulted in a change in mean $SUV_{total}$ from 264 to 280, with little change in the correlation between $SUV_{total}$ and stimulated Tg (ρ changes from 0.65 to 0.64 in the low-intermediate risk group, from 0.61 to 0.60 in the high-intermediate risk group and remained unchanged in the high-risk group).

However, a strong significant correlation was observed between the total lesion uptake values obtained using the two thresholds (ρ=1.00, *p*-value <0.001), indicating that our segmentation method is not highly sensitive to the set threshold (**Figure 8**). We chose to focus on the 0.5 SUV threshold, as it is less affected by background signal.

The second limitation of our study is that Tg measurements may be subject to variability, as they depend on the radioimmunoassay or immunometric assay used [16, 36]. Due to the retrospective nature of the study, patients' Tg levels were obtained from clinical records, and therefore, could have been measured at different hospitals or clinics. Furthermore, a considerable number of patients in our study had Tg levels below the detectable limit (0.2 pmol/L or 0.7 pmol/L depending on the laboratory). Consequently, we did not perform an analysis of the association between non-stimulated (basal) Tg and thyroid remnant activity, as 41% of patients had undetectable Tg levels.

Lastly, it is known that Tg levels measured immediately post-surgery may not be reliable, as surgical manipulation of the thyroid gland releases significant amounts of Tg into the systemic circulation. At our institution, the typical interval between surgery and radioiodine ablation is a

median of 77.5 days (mean 89.2±49.1), which is unlikely to contribute significantly to Tg levels in most patients, although possible residual inflammatory processes may persist in some patients.

In conclusion, we demonstrated the feasibility of quantifying thyroid remnant uptake on post-ablation therapy SPECT/CT in patients with thyroid cancer. The quantification methodology could be helpful in the quantification of tumor burden in follow-up diagnostic studies. We examined the direct association between thyroid remnant activity and Tg levels during radioiodine ablation which demonstrated a moderate correlation in the low-intermediate and high-intermediate risk groups. However, the correlation in the high-risk group was weak, presumably due to factors including micro-metastases, thyroid bed/remnant inflammation, and high-risk histological subtypes. Given that both imaging findings and Tg measurements are influenced by multiple factors, as evidenced by the outliers observed in our study, both thyroid scans and Tg measurements should be used for patient surveillance.

## Disclosure of conflict of interest

None.

## Abbreviations

Tg, thyroglobulin; TgAb, thyroglobulin antibody; RAI, radioactive iodine; SPECT, single photon emission computed tomography; SUV, standard uptake value; OSEM, ordered subset expectation maximization.

**Address correspondence to:** Dr. Wanzhen Zeng, Division of Nuclear Medicine and Molecular Imaging, Department of Medicine, University of Ottawa, 1053 Carling Ave., Ottawa, Ontario K1Y 4E9, Canada. Tel: 613-737-8528; E-mail: wzeng@toh.ca

## References

[1] Avram AM, Giovanella L, Greenspan B, Lawson SA, Luster M, Van Nostrand D, Peacock JG, Ovčariček PP, Silberstein E, Tulchinsky M, Verburg FA and Vrachimis A. SNMMI procedure standard/EANM practice guideline for nuclear medicine evaluation and therapy of differentiated thyroid cancer: abbreviated version. J Nucl Med 2022; 63: 15N-35N.

[2] Haugen BR, Alexander EK, Bible KC, Doherty GM, Mandel SJ, Nikiforov YE, Pacini F, Randolph GW, Sawka AM, Schlumberger M, Schuff KG, Sherman SI, Sosa JA, Steward DL, Tuttle RM and Wartofsky L. 2015 American thyroid association management guidelines for adult patients with thyroid nodules and differentiated thyroid cancer: the american thyroid association guidelines task force on thyroid nodules and differentiated thyroid cancer. Thyroid 2016; 26: 1-133.

[3] Spencer C, LoPresti J and Fatemi S. How sensitive (second-generation) thyroglobulin measurement is changing paradigms for monitoring patients with differentiated thyroid cancer, in the absence or presence of thyroglobulin autoantibodies. Curr Opin Endocrinol Diabetes Obes 2014; 21: 394-404.

[4] Hocevar M, Auersperg M and Stanovnik L. The dynamics of serum thyroglobulin elimination from the body after thyroid surgery. Eur J Surg Oncol 1997; 23: 208-210.

[5] Mazzaferri EL and Kloos RT. Clinical review 128: current approaches to primary therapy for papillary and follicular thyroid cancer. J Clin Endocrinol Metab 2001; 86: 1447-1463.

[6] Doi SA, Woodhouse NJ, Thalib L and Onitilo A. Ablation of the thyroid remnant and I-131 dose in differentiated thyroid cancer: a meta-analysis revisited. Clin Med Res 2007; 5: 87-90.

[7] Hackshaw A, Harmer C, Mallick U, Haq M and Franklyn JA. 131I activity for remnant ablation in patients with differentiated thyroid cancer: a systematic review. J Clin Endocrinol Metab 2007; 92: 28-38.

[8] Bachelot A, Cailleux AF, Klain M, Baudin E, Ricard M, Bellon N, Caillou B, Travagli JP and Schlumberger M. Relationship between tumor burden and serum thyroglobulin level in patients with papillary and follicular thyroid carcinoma. Thyroid 2002; 12: 707-711.

[9] Tamilia M, Al-Kahtani N, Rochon L, Hier MP, Payne RJ, Holcroft CA and Black MJ. Serum thyroglobulin predicts thyroid remnant ablation failure with 30 mCi iodine-131 treatment in patients with papillary thyroid carcinoma. Nucl Med Commun 2011; 32: 212-220.

[10] Hommel I, Pieters GF, Rijnders AJ, van Borren MM and de Boer H. Success rate of thyroid remnant ablation for differentiated thyroid cancer based on 5550 MBq post-therapy scan. Neth J Med 2016; 74: 152-157.

[11] Cherk MH, Kalff V, Yap KS, Bailey M, Topliss D and Kelly MJ. Incidence of radiation thyroiditis and thyroid remnant ablation success rates following 1110 MBq (30 mCi) and 3700 MBq (100 mCi) post-surgical 131I ablation therapy for differentiated thyroid carcinoma. Clin Endocrinol (Oxf) 2008; 69: 957-962.

[12] Park HJ, Jeong GC, Kwon SY, Min JJ, Bom HS, Park KS, Cho SG, Kang SR, Kim J, Song HC, Chong A and Yoo SW. Stimulated serum thyroglobulin level at the time of first dose of radioactive iodine therapy is the most predictive factor for therapeutic failure in patients with papillary thyroid carcinoma. Nucl Med Mol Imaging 2014; 48: 255-261.

[13] Park HJ, Min JJ, Bom HS, Kim J, Song HC and Kwon SY. Early stimulated thyroglobulin for response prediction after recombinant human thyrotropin-aided radioiodine therapy. Ann Nucl Med 2017; 31: 616-622.

[14] Hwang SH, Jo K, Cha J, Kang CG, Wang J, Cho H, Kang WJ and Cho A. Correlation between remnant thyroid gland I-131 uptake and serum thyroglobulin levels: can we rely on I-131 whole body scans? Cancer Imaging 2024; 24: 21.

[15] Ringel MD and Nabhan F. Approach to follow-up of the patient with differentiated thyroid cancer and positive antithyroglobulin antibodies. J Clin Endocrinol Metab 2013; 98: 3104-3110.

[16] Clark P and Franklyn J. Can we interpret serum thyroglobulin results? Ann Clin Biochem 2012; 49: 313-322.

[17] Ciappuccini R, Hardouin J, Heutte N, Vaur D, Quak E, Rame JP, Blanchard D, de Raucourt D and Bardet S. Stimulated thyroglobulin level at ablation in differentiated thyroid cancer: the impact of treatment preparation modalities and tumor burden. Eur J Endocrinol 2014; 171: 247-252.

[18] Carvalho MR, Ferreira TC and Leite V. Evaluation of whole-body retention of iodine-131 (131I) after postoperative remnant ablation for differentiated thyroid carcinoma - thyroxine withdrawal versus rhTSH administration: a retrospective comparison. Oncol Lett 2012; 3: 617-620.
[19] Andresen NS, Buatti JM, Tewfik HH, Pagedar NA, Anderson CM and Watkins JM. Radioiodine ablation following thyroidectomy for differentiated thyroid cancer: literature review of utility, dose, and toxicity. Eur Thyroid J 2017; 6: 187-196.
[20] Cancer Care Ontario. Differentiated thyroid cancer treatment pathway map. September 2019.
[21] Schober P, Boer C and Schwarte LA. Correlation coefficients: appropriate use and interpretation. Anesth Analg 2018; 126: 1763-1768.
[22] Webb RC, Howard RS, Stojadinovic A, Gaitonde DY, Wallace MK, Ahmed J and Burch HB. The utility of serum thyroglobulin measurement at the time of remnant ablation for predicting disease-free status in patients with differentiated thyroid cancer: a meta-analysis involving 3947 patients. J Clin Endocrinol Metab 2012; 97: 2754-2763.
[23] Bernier MO, Morel O, Rodien P, Muratet JP, Giraud P, Rohmer V, Jeanguillaume C, Bigorgne JC and Jallet P. Prognostic value of an increase in the serum thyroglobulin level at the time of the first ablative radioiodine treatment in patients with differentiated thyroid cancer. Eur J Nucl Med Mol Imaging 2005; 32: 1418-1421.
[24] Lim ES, Shah SG, Waterhouse M, Akker S, Drake W, Plowman N, Berney DM, Richards P, Adams A, Nowosinska E, Brennan C and Druce M. Impact of thyroiditis on 131I uptake during ablative therapy for differentiated thyroid cancer. Endocr Connect 2019; 8: 571-578.
[25] Kwon H, Choi JY, Moon JH, Park HJ, Lee WW and Lee KE. Effect of Hashimoto thyroiditis on low-dose radioactive-iodine remnant ablation. Head Neck 2016; 38 Suppl 1: E730-5.
[26] Stevic I, Dembinski TC, Pathak KA and Leslie WD. Transient early increase in thyroglobulin levels post-radioiodine ablation in patients with differentiated thyroid cancer. Clin Biochem 2015; 48: 658-661.
[27] Tsang JF, Levin DP and Leslie WD. Thyroglobulin flare response after radioiodine ablation in 2 patients with differentiated thyroid cancer. Clin Nucl Med 2015; 40: 421-422.
[28] Zampella E, Klain M, Pace L and Cuocolo A. PET/CT in the management of differentiated thyroid cancer. Diagn Interv Imaging 2021; 102: 515-523.
[29] Donohoe KJ, Aloff J, Avram AM, Bennet KG, Giovanella L, Greenspan B, Gulec S, Hassan A, Kloos RT, Solórzano CC, Stack BC Jr, Tulchinsky M, Tuttle RM, Van Nostrand D and Wexler JA. Appropriate use criteria for nuclear medicine in the evaluation and treatment of differentiated thyroid cancer. J Nucl Med 2020; 61: 375-396.
[30] Nascimento C, Borget I, Al Ghuzlan A, Deandreis D, Hartl D, Lumbroso J, Berdelou A, Lepoutre-Lussey C, Mirghani H, Baudin E, Schlumberger M and Leboulleux S. Postoperative fluorine-18-fluorodeoxyglucose positron emission tomography/computed tomography: an important imaging modality in patients with aggressive histology of differentiated thyroid cancer. Thyroid 2015; 25: 437-444.
[31] IAEA-TECDOC-1608. Nuclear medicine in thyroid cancer management: a practical approach. March 2009.
[32] Ma C, Kuang A, Xie J and Ma T. Possible explanations for patients with discordant findings of serum thyroglobulin and 131I whole-body scanning. J Nucl Med 2005; 46: 1473-1480.
[33] Zeuren R, Biagini A, Grewal RK, Randolph GW, Kamani D, Sabra MM, Shaha AR and Tuttle RM. RAI thyroid bed uptake after total thyroidectomy: a novel SPECT - CT anatomic classification system. Laryngoscope 2015; 125: 2417-2424.
[34] Caballero-Calabuig E, Cano-Terol C, Sopena-Monforte R, Reyes-Ojeda D, Abreu-Sánchez P, Ferrer-Rebolleda J, Sopena-Novales P, Plancha-Mansanet C and Félix-Fontestad J. Influence of the thyroid remnant in the elevation of the serum thyroglobulin after thyroidectomy in differentiated thyroid carcinoma. Importance of the diagnostic iodine total-body scanning. Eur J Nucl Med Mol Imaging 2008; 35: 1449-1456.
[35] Silva F, Martin RJ, Figueroa J, Rincón F and Román D. Variability of serum thyroglobulin levels in post- thyroidectomy patients with well-differentiated thyroid cancer: the ATA guidelines. P R Health Sci J 2016; 35: 142-146.
[36] Spencer C and Fatemi S. Thyroglobulin antibody (TgAb) methods - Strengths, pitfalls and clinical utility for monitoring TgAb-positive patients with differentiated thyroid cancer. Best Pract Res Clin Endocrinol Metab 2013; 27: 701-712.